

# The impact of coniferous forest temperature on incoming longwave radiation to melting snow

John W. Pomeroy,<sup>1\*</sup> Danny Marks,<sup>2</sup> Tim Link,<sup>3</sup> Chad Ellis,<sup>1</sup> Janet Hardy,<sup>4</sup> Aled Rowlands<sup>5</sup>  
and Raoul Granger<sup>6</sup>

<sup>1</sup> Centre for Hydrology, University of Saskatchewan, Saskatoon, Sask, Canada, S7N 5C8

<sup>2</sup> USDA Agricultural Research Service, Northwest Watershed Research Center, Boise, ID, USA

<sup>3</sup> College of Forest Resources, University of Idaho, Moscow, ID, USA

<sup>4</sup> US Army Cold Regions Research and Engineering Laboratory, Hanover, NH, USA

<sup>5</sup> Institute of Geography and Earth Sciences, Aberystwyth University, Aberystwyth, Wales

<sup>6</sup> Environment Canada, Saskatoon, Sask, Canada, S7N 3H5

## Abstract:

Measurements were conducted in coniferous forests of differing density, insolation and latitude to test whether air temperatures are suitable surrogates for canopy temperature in estimating sub-canopy longwave irradiance to snow. Air temperature generally was a good representation of canopy radiative temperature under conditions of low insolation. However during high insolation, needle and branch temperatures were well estimated by air temperature only in relatively dense canopies and exceeded air temperatures elsewhere. Tree trunks exceeded air temperatures in all canopies during high insolation, with the relatively hottest trunks associated with direct interception of sunlight, sparse canopy cover and dead trees. The exitance of longwave radiation from these relatively warm canopies exceeded that calculated assuming canopy temperature was equal to air temperature. This enhancement was strongly related to the extinction of shortwave radiation by the canopy. Estimates of sub-canopy longwave irradiance using either two-energy source or two thermal regime approaches to evaluate the contribution of canopy longwave exitance performed better than did estimates that used only air temperature and sky view. However, there was little evidence that such corrections are necessary under cloudy or low solar insolation conditions. The longwave enhancement effect due to shortwave extinction was important to sub-canopy longwave irradiance to snow during clear, sunlit conditions. Longwave enhancement increased with increasing solar elevation angle and decreasing air temperature. Its relative importance to longwave irradiance to snow was insensitive to canopy density. As errors from ignoring enhanced longwave contributions from the canopy accumulate over the winter season, it is important for snow energy balance computations to include the enhancement in order to better calculate snow internal energy and therefore the timing and magnitude of snowmelt and sublimation. Copyright © 2009 John Wiley & Sons, Ltd.

KEY WORDS snowmelt; longwave radiation; forest temperature; shortwave radiation; transmissivity; pine forest; rocky mountains; CLPX

Received 8 June 2008; Accepted 9 March 2009

## INTRODUCTION

The warming, melting and ablation of sub-canopy snow is a crucial event in the annual cycle of a cold regions forest and governs the hydrology and atmospheric interaction of the forest. The timing and spatial distribution of snow meltwater production controls the meltwater hydrograph shape, peak and duration, initiates soil thawing and transpiration and governs the decay of surface albedo. Radiation is usually the primary source of energy for snowmelt under forest canopies (Link and Marks, 1999) because turbulent transfer is strongly attenuated by the canopy structure (Harding and Pomeroy, 1996; Pomeroy and Granger, 1997; Marks *et al.*, 2008). Both short and longwave radiation are important to snowmelt (Sicart *et al.*, 2004), with the relative contribution from each depending on snowcover albedo, cloudiness and canopy

density. Whilst shortwave radiation under forest canopies has received much recent attention from both observations and model development (Wilson and Petzold, 1973; Pomeroy and Dion, 1996; Davis *et al.*, 1997; Hardy *et al.*, 1997; Ni *et al.*, 1997; Nijssen and Lettenmaier, 1999; Gryning *et al.*, 2001; Hardy *et al.*, 2004; Link *et al.*, 2004; Ellis and Pomeroy, 2007; Pomeroy *et al.*, 2008), less attention has been paid to longwave radiation effects on snowmelt except for the case of sparse canopies (Woo and Giebrecht, 2000). It is generally assumed that longwave radiation to snow can be partitioned between that deriving from a sky view component (Price and Petzold, 1984) and that deriving from a canopy view component with an effective temperature equal to air temperature.

It is the purpose of this paper to examine for continental forests during the premelt and snowmelt periods whether

1. the canopy temperature can be approximated by the air temperature,

\* Correspondence to: John W. Pomeroy, Centre for Hydrology, University of Saskatchewan, Saskatoon, Sask, Canada, S7N 5C8.  
E-mail: john.pomeroy@usask.ca

2. extinction of shortwave radiation in the canopy is a significant mechanism of additional warming of the canopy,
3. canopy warming enhances longwave irradiance to snow.

For cases when the canopy temperature exceeds the air temperature, strategies to estimate the effect of enhanced canopy temperatures on snowmelt radiation under forest canopies will be described and tested.

### THEORY

A major source of net radiation under forest canopies is incoming longwave radiation (Sicart *et al.*, 2004). This is usually estimated by segregation of the component passing through the canopy from the sky ( $L_o \downarrow$ ) from the component emitted by the canopy itself ( $L_c \downarrow$ ) using the sky view factor,  $V_f$ , where

$$L \downarrow = V_f L_o \downarrow + (1 - V_f) L_c \downarrow \quad (1)$$

Using the Stefan–Boltzmann equation and assuming that sky and canopy are grey bodies, i.e. the sub-canopy longwave irradiance can be estimated from the temperatures of the emitting sources by,

$$L \downarrow = V_f (\varepsilon_{\text{sky}} \sigma T_{\text{sky}}^4) + (1 - V_f) (\varepsilon_{\text{can}} \sigma T_{\text{can}}^4) \quad (2)$$

where  $\varepsilon$  is a dimensionless effective emissivity for sky or canopy (can),  $\sigma$  is the Stefan–Boltzmann constant ( $5.67 \times 10^{-8} \text{ W m}^{-2} \text{ K}^{-4}$ ) and  $T$  represents an effective temperature (K) of sky or canopy given the form and assumptions of Equation 2. The emissivity is also effective because reflectance of longwave radiation is not explicitly addressed in Equation 2 and because air temperature near the surface is often substituted for the temperature of the radiating portion of the atmosphere. Many models (Marks *et al.*, 1999; Pomeroy *et al.*, 2007) make further simplification of Equation 2 by assuming that sky emissions of longwave occur in the lower atmosphere and can be represented by the air temperature and that the temperature of the canopy can be approximated by the air temperature,  $T_a$  so that longwave irradiance is a function of the two variables: air temperature and sky emissivity and two parameters: sky view factor and canopy emissivity, so that;

$$L \downarrow = \sigma T_a^4 (V_f \varepsilon_{\text{air}} + (1 - V_f) \varepsilon_{\text{can}}) \quad (3)$$

Sicart *et al.* (2006) have shown a method for estimating  $\varepsilon_{\text{sky}}$  during snowmelt in western and northern Canada from standard atmospheric variables and a measure of cloudiness, whilst many sources (e.g. Oke, 1987) cite the effective emissivity of forest canopy  $\varepsilon_{\text{can}} = 0.98$  (slightly higher than the actual emissivity).

A very important assumption of Equation 3 is that  $T_a = T_{\text{sky}} = T_{\text{can}}$ . Correct estimation of canopy temperature is essential to the calculation of forest longwave exitance, which is the sum of emission and reflection

of longwave radiation. As Sicart *et al.* (2004) showed, whilst in low sun angle, cloudy environments, or in dense forest where tree stems are not frequently sunlit, there is little opportunity for the canopy temperature to differ from air temperature. However in sunny environments where direct insolation to tree trunks, branches and needles occurs, warming of canopy elements by shortwave radiation may result in enhanced longwave exitance from the canopy. It is therefore possible that in some cases the key assumption behind Equation 3 is not met. This is a common feature of sunlit vegetation and is the reason why vegetation canopies can be a source of sensible heat in winter conditions (Harding and Pomeroy, 1996; Gryning *et al.*, 2001; Pomeroy *et al.*, 2006). Rowlands *et al.* (2002) show that canopy temperatures over melting snow can greatly exceed air temperatures in sunny late winter conditions in the Rocky Mountains of Colorado.

Some atmospheric models such as Canadian Land Surface Scheme (CLASS) (Verseghy and McFarlane, 1993) include canopy energetic formulations to resolve a canopy temperature. These techniques have been incorporated into a few hydrological models (Parviainen and Pomeroy, 2000), but in general, hydrological models have not gone into such detailed energetics calculations because of over-parameterisation and resulting parameter uncertainty. An alternative method is to assume that some portion of shortwave energy absorbed by a canopy is emitted downwards as longwave energy and contributes to sub-canopy longwave irradiance. Sub-canopy longwave emission due to shortwave heating of canopy  $L \downarrow_H$  is then a function of the amount of shortwave energy extinguished in the canopy  $K^*_H$ , where

$$L \downarrow_H = B K^*_H \quad (4)$$

and  $B$  is a dimensionless shortwave to longwave transfer efficiency function. Assuming that only first order multiple sub-canopy reflection is important and that  $K^*_H$  is defined for a canopy height,  $H$ , then,

$$K^*_H = K \downarrow - K \uparrow - K_c \downarrow + K_c \uparrow \quad (5)$$

Noting that  $K \uparrow = K \downarrow \alpha_c$ , where  $\alpha_c$  is above canopy albedo,  $K_c \downarrow = K \downarrow \tau$ , where  $\tau$  is the canopy transmittance to shortwave radiation, and  $K_c \uparrow = K_c \downarrow \alpha_s = K \downarrow \tau \alpha_s$ , where  $\alpha_s$  is the snow albedo, then,

$$K^*_H = K \downarrow [1 - \alpha_c - \tau(1 - \alpha_s)] \quad (6)$$

Values of  $\alpha_c$  ranging from 0.08 to 0.18 have been reported by Pomeroy and Dion (1996) and Betts and Ball (1997) for boreal forests. Melloh *et al.* (2002) have investigated sub-canopy snowpack albedo,  $\alpha_s$ , over a winter and found it in the range 0.8–0.9.

To find  $\tau$ , Pomeroy and Dion (1996) derived a simple algorithm for relatively continuous canopies from geometric optics, (van de Hulst, 1980);

$$\tau = e^{-\frac{Q_{\text{ext}} LAI'}{\sin(\beta)}} \quad (7)$$

where  $Q_{\text{ext}}$  is the extinction efficiency,  $LAI'$  is the effective winter plant area index, and  $\beta$  is the solar elevation angle above the horizon. Pomeroy and Dion (1996) found that the extinction efficiency was a function of daily mean solar angle, because of the relatively horizontal orientation of small canopy elements and gap configurations (most canopies have some gaps).

## METHODS

Experiments to examine the canopy temperatures, shortwave extinction and effects on longwave irradiance to snow under canopies were conducted in level Rocky Mountain lodgepole pine stands in the US Forest Service, Fraser Experimental Forest near Fraser, Colorado, USA (39°59'N; 105°59'W; 2780 m above sea level—Hardy *et al.* 2004 and Pomeroy *et al.* 2008 for detailed site description) and in Marmot Creek Research Basin in the Kananaskis valley of Alberta, Canada (50°57'N, 115°09'W; 1530 m above sea level—Ellis and Pomeroy, 2007 for detailed site description). The Fraser sites consisted of a uniform lodgepole pine stand and an adjacent discontinuous, highly heterogeneous pine stand. The uniform pine had relatively even spacing between trees from thinning. Trees in the discontinuous site were of mixed species (predominantly lodgepole pine with some Englemann spruce and subalpine fir) with heterogeneous spacing between trees. The Marmot site was a very mature, dense, natural lodgepole pine stand with variable spacing between trees. Data used to evaluate shortwave extinction as a function of leaf area index and solar angle in pine were collected in a mature boreal jack pine canopy near Waskesiu, Saskatchewan, Canada (53°52'N; 106°08'W; 540 m above sea level) that was originally described by Pomeroy and Dion (1996). Data collection at Fraser focussed on a 3-day period during the NASA Cold Land Processes Experiment (CLPX), Hardy *et al.* (2008) Intensive Observation Period 2 (IOP2) from 27 to 29 March 2002 (days 86–88). The snowpack was isothermal and actively melting during this period and had become patchy in the discontinuous pine stand. At Marmot Creek, data collection focussed on 15–18 March 2005 (days 74–77) when a shallow snowpack was isothermal and actively melting. Weather conditions for the experimental days are summarized in Table I. At all sites, radiometers were inspected several times a day and cleaned if required

to prevent frost accumulation, however the weather conditions were ideal for these measurements and there was very little frost and no snowfall during the study.

Narrow-beam thermal infrared radiometers (*Exergen* infrared thermocouples (IRTC)) and hypodermic needle style thermocouples (*Omega* HYP-0 TC) controlled by Campbell Scientific 23X dataloggers were used to measure surface temperatures of main tree trunks, small branches and pine needles. In the uniform stand at Fraser and at Marmot Creek, IRTCs were used to measure needle, branch and trunk temperatures as there was a continuous view of the surfaces in question and the narrow-beam view provided an ideal spatially averaged measurement. At the Fraser uniform stand, IRTCs measured the trunk of a living pine (~1 m above the snow) and the needles-branches of several trees, viewed obliquely from below. At Marmot Creek, IRTCs were placed to measure needle-branch temperature and trunk temperature from both north and south sides and measurements were averaged. In the discontinuous stand at Fraser there were insufficient continuous, uniform fields of view for the IRTCs and so TCs were used to gather point temperature measurements. A TC inserted via a hypodermic needle (*Omega* HYP-0, 0.2 mm), threaded through the exterior of rough bark, measured the skin temperature of a dead tree trunk that was well exposed to the sun. This hypodermic TC received some direct solar radiation and had a continuous contact surface conducting heat from the trunk. Fine wire TCs (0.13 mm) were attached by thread to the surface of needles or branches to measure their surface temperatures in trees that were well exposed to the sun. These fine wire TCs received some direct solar radiation and had a continuous contact surface with the branch or needles. An intercomparison of the IRTC and hypodermic TC temperature measurements where the TC was attached to the outside of a trunk at Fraser showed a mean difference  $TC - IRTC = -0.089^\circ\text{C}$  with an RMSD (root mean square difference) =  $0.839^\circ\text{C}$  from 865 measurements in sun and shade. This mean difference is within the measurement error of thermocouples in this environment.

Air temperatures above (18 m above ground) and below (3 m above ground) the uniform canopy at Fraser were measured using shielded *Vaisala* HMP35 hygrometers. Air temperatures at 2 m above ground were measured using a shielded *Vaisala* HMP45CF at Marmot Creek.

Table I. Weather conditions and mean shortwave irradiance for each day at each site

Date	Day	Location	Conditions	Minimum air temperature ( $^\circ\text{C}$ )	Maximum air temperature ( $^\circ\text{C}$ )	Mean shortwave irradiance ( $\text{W m}^{-2}$ )
27 March	86	Fraser	Overcast	-6.8	3.8	115
28 March	87	Fraser	Clear sky	-3.1	6.5	248
29 March	88	Fraser	Clear sky	-7.0	6.2	263
15 March	74	Marmot	Partly cloudy	-6.7	3.8	143
16 March	75	Marmot	Overcast	-9.3	0.7	100
17 March	76	Marmot	Mostly clear	-10.7	-2.8	173
18 March	77	Marmot	Partly cloudy	-10.2	-7.1	159

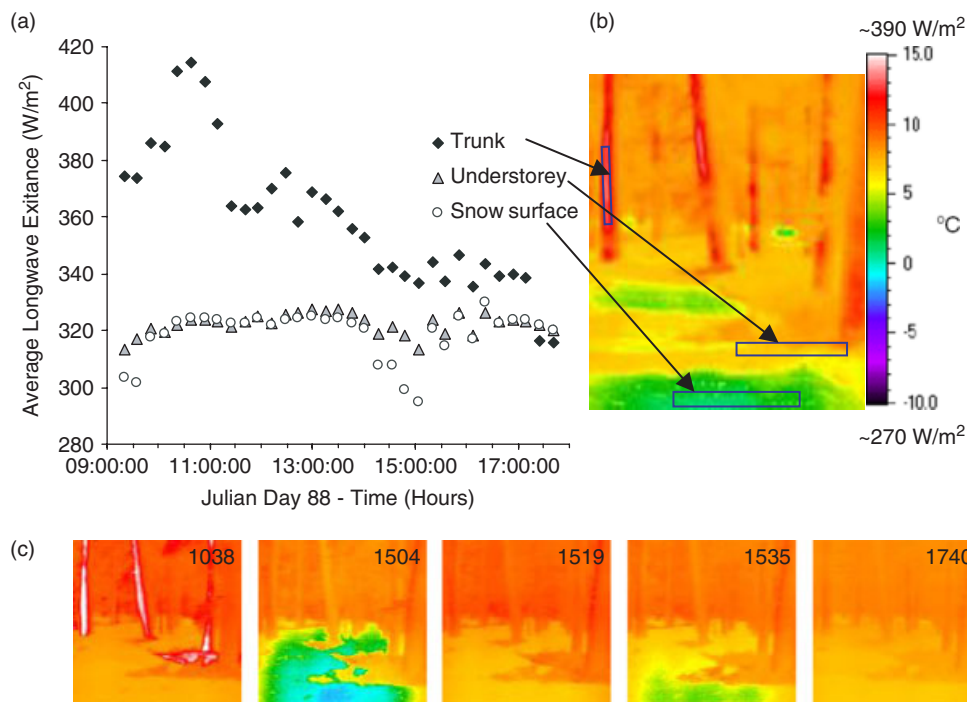


Figure 1. Thermograph measurements of thermal structure from the discontinuous stand, Fraser. Three areas within the scene were identified (b) and mean temperature for each was calculated. The regions of interest focused on snow, canopy understorey and trunk. Mean temperatures, converted to  $W/m^2$ , are shown in (a). The spatial variation in temperature throughout day 88 can be seen in the selection of thermographs (c)

At Fraser, small arrays of four *Eppley* PIR pyrgeometers (previously cross calibrated) were used to measure irradiance under the uniform and discontinuous stands. In the uniform stand, pyrgeometers were located by selecting a random distance and angle from a central distribution point. In the discontinuous stand, pyrgeometer placement also considered proximity to tree trunks and placement in canopy gaps so that one pyrgeometer was in a canopy gap and one was placed within 1.5 m of a tree and near to other trees. A *Kipp and Zonen* CG3 pyrgeometer and CG1 pyranometer on a 20 m tower provided above canopy reference irradiance for Fraser. At Marmot Creek, arrays of 10 *Eppley* PIR and two *Kipp and Zonen* CG1 pyrgeometers were placed randomly. A reference site was established in a large clearing near this stand for measuring incoming longwave and shortwave from open sky using CG1 and CG3 radiometers. Digital thermograms were collected at Fraser using a thermoelectric thermal infrared imaging radiometer (*Infrared Solutions*) that had been modified to operate over the temperature range from  $-27$  to  $+20$  °C, with a spectral range of 8 to 12  $\mu m$ , absolute accuracy of  $1.2$  °C and differential accuracy of  $0.1$  °C. Each digital thermogram was  $120 \times 120$  pixels. The instrument was mounted on a tripod and controlled from a linked laptop computer to obtain an image of canopy needle-branches, trunk and surface snow every 15 min.

#### FOREST CANOPY AND AIR TEMPERATURES

The thermal structure of the sub-canopy environment was first examined using observations from the thermal

infrared imaging radiometer (Figure 1). These images allow for visualization and interpretation of thermal structure under the discontinuous canopy. The temperatures shown were all calculated using an emissivity of 1.0 and actual emissivities vary slightly from this value. The area shown in Figure 1b was under intense solar irradiation in the morning of day 88, when the index surface temperatures on the trunk reached nearly  $20$  °C. Afternoon shading resulted in the index temperature distribution narrowing. Three elements of the scene were quantified. The ground elements (shrubs and snow) were restrained in their index temperature range despite similar radiative outputs. This reflects both differing actual emissivities and snow temperatures that were restricted by the  $0$  °C limit upon which further energy goes into phase change rather than an increase in temperature. The 'hot spots' evident on the trunk play an important role in snow ablation as a bare patch developed near the tree trunk. This is consistent with observations by Faria *et al.* (2000) that showed more rapid snow ablation near the trunk in such environments.

Because of the variable and elevated canopy temperatures seen in Figure 1, the assumption that  $T_a = T_{can}$  was tested. To test this, canopy temperatures measured using the IRTC and TC in the continuous and discontinuous stands at Fraser and at Marmot were compared to air temperatures measured under the homogeneous canopy and, at Fraser, above the canopy (Figure 2).

The atmosphere at Fraser was generally stable with colder temperatures below canopy (3 m height) than above (18 m height). Temperature depressions below the homogeneous canopy were  $\sim 1$  °C during all daytime

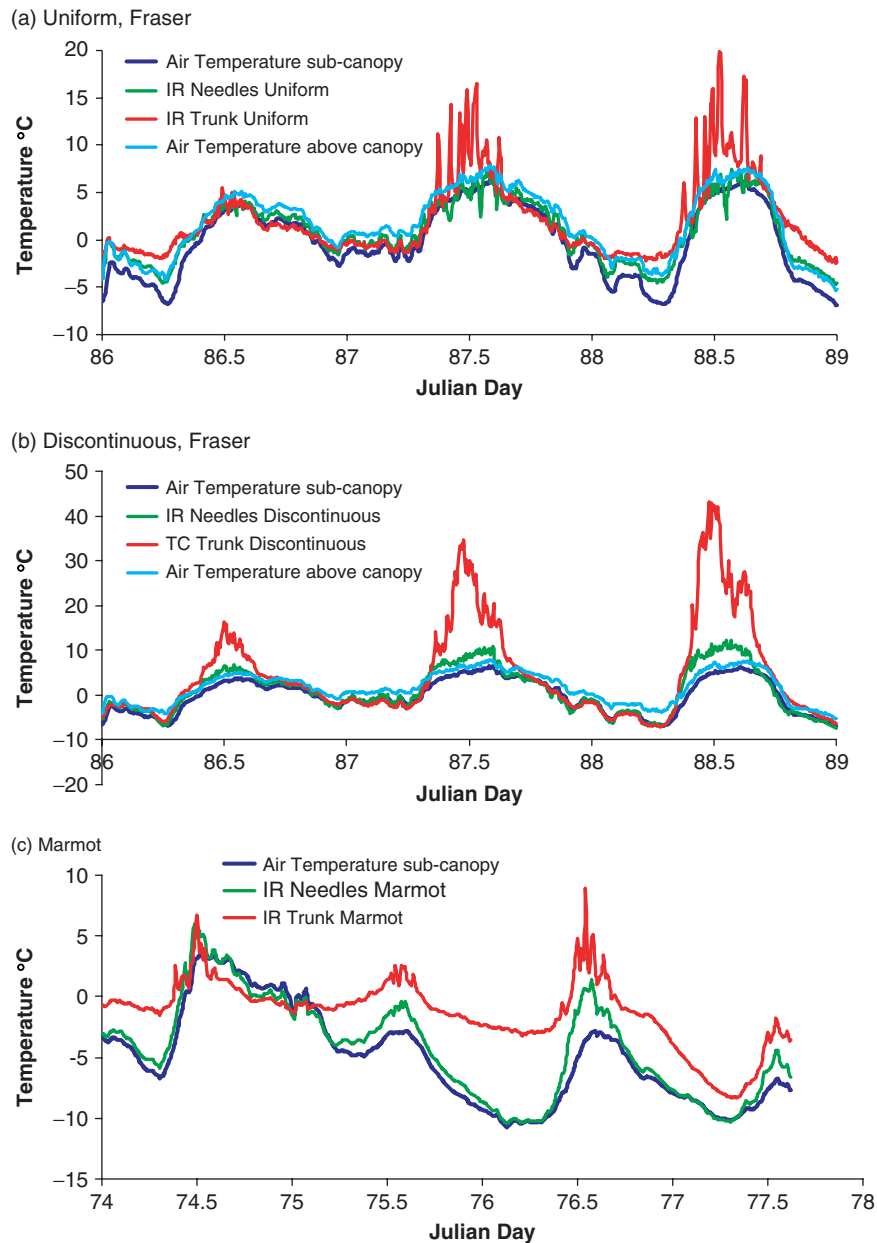


Figure 2. Needle-branch, trunk and air temperatures in the Fraser (a) uniform and (b) discontinuous stands and at (c) Marmot Creek during the longwave radiation experiments

periods and on cloudy nights and up to  $3^{\circ}\text{C}$  on clear nights, with an overall mean of  $1.9^{\circ}\text{C}$  and a RMS (root mean square) difference of  $2.1^{\circ}\text{C}$ . Only sub-canopy air temperature measurements were available from Marmot and so stability was not assessed there.

At both Fraser and Marmot, substantial differences between sub-canopy air, needle-branch and trunk temperatures were evident over all periods of analysis at all sites. Needle-branch and air temperatures generally matched each other well (as close as  $0.1^{\circ}\text{C}$ ) at night and on cloudy days (days 86 Fraser, 74 Marmot); only where inversions developed at night (early morning day 88 Fraser) did sub-canopy air temperatures drop below needle-branch temperatures (by up to  $1.5^{\circ}\text{C}$ ). Trunk temperatures generally remained warmer than needle-branch and air temperatures at night, with strongest effects ( $4.5$  to  $7.0^{\circ}\text{C}$ ) on

clear nights. The living trunks at the uniform Fraser stand and the Marmot stand remained warmer at night than the dead trunk in the discontinuous Fraser stand despite similar diameters. This suggests a hypothesis that water stored in the trunks of living trees could exert a control on heat storage and hence on trunk cooling at night and warming during sunlit periods, however this hypothesis could not be explored with this experiment. During the day the trunks in all stands became substantially warmer than air with the largest warming on clear days. The most extreme relative heating was for the well-exposed dead trunk in the discontinuous Fraser stand which reached a temperature of over  $43^{\circ}\text{C}$  during a clear, high sun period when air temperature was  $\sim 5^{\circ}\text{C}$ , a difference of  $38^{\circ}\text{C}$ . Differences were smaller but still substantial for the living trunks and needle-branches in the Marmot and uniform Fraser

stands, which were 5–15 °C warmer than air temperature when sunlit. In contrast, needle-branches in the uniform stand tracked sub-canopy air temperature rather closely (normally within 0.5 °C) during all days. On cloudy days, canopy-air temperature differences were subdued except in the Fraser discontinuous stand where the trunk was up to 12 °C warmer than air. Above canopy air temperatures were sometimes a good match for continuous stand needle-branch temperatures but otherwise were not well matched by any canopy elements.

The colder air under forest canopies has important implications for canopy temperature calculations because standard meteorological stations in forest clearings are influenced by both above and below-canopy air. In large clearings, it is expected that above canopy temperatures will dominate; however, a problem in interpreting clearing air temperatures is that the degree of mixing between sub-canopy and above canopy air in a clearing will vary with wind speed, stability, clearing size and exposure to wind (Taylor *et al.*, 1998). In specialized forest snowmelt studies, there are sometimes sub-canopy air temperature measurements made, but in atmospheric model snowmelt calculations the 'reference' lower atmospheric layer is usually well above the canopy. The choice of measurement height is clearly important and a possible cause of errors in estimating canopy temperature.

#### LONGWAVE EXITANCE

The longwave exitance (emission and reflection) from various sources to the sub-canopy snow was measured using above canopy pyrgeometers (sky), and estimated using IRTC narrow-beam radiometers (canopy and trunk), hygrometers (air) and TC (trunk and needle-branches). Canopy and air temperatures were converted to exitance in  $\text{W m}^{-2}$  using the Stefan–Boltzmann equation and an effective emissivity of 0.98 (Oke, 1987). Calculations of exitance from air with such a high emissivity are an index to the exitance from a forest surface at the same temperature as the sub-canopy air. As shown in Table II and Figure 3 the major difference was that between exitances from the sky and that from canopy elements. This difference between sky and canopy was greatest for clear periods, (day 87, 88 and mid-day 76) where it was on the order of  $100 \text{ W m}^{-2}$ . However, on some cloudy nights the sky and canopy exitances were extremely well matched.

Table II and Figure 3 show that the needle-branch and air temperature-based exitances generally agreed well in the uniform Fraser stand with the needle-branch exitance being slightly higher than that from surfaces at the air temperature. The largest differences ( $18 \text{ W m}^{-2}$ , needle-branch > air) were on clear nights when strong inversions occurred. Needle-branch and air temperature-based exitances were in excellent agreement with the Marmot stand and the discontinuous Fraser stand at night and on cloudy days but needle-branch exitances exceeded air temperatures during sunlit periods with the largest differences of  $20\text{--}34 \text{ W m}^{-2}$  occurring during clear days.

Table II. Differences between the longwave exitance from canopy elements and sub-canopy air with a hypothetical effective emissivity of 0.98

	RMS difference $\text{W m}^{-2}$	Maximum difference $\text{W m}^{-2}$	Mean difference $\text{W m}^{-2}$
<i>Needle-branch-air</i>			
Fraser homogeneous	6.3	18.0	4.7
Fraser discontinuous	10.2	34.5	5.6
Marmot homogeneous	5.5	20.2	3.2
<i>Trunk-air</i>			
Fraser homogeneous	15.5	76.1	10.2
Fraser discontinuous	50.0	225.8	24.3
Marmot homogeneous	19.8	58.1	15.8

The difference shows the error in assuming that canopy air temperature is a substitute for actual surface temperatures in the canopy.

As a result of variable needle-branch warming during the day at Marmot and Fraser (and cold sub-canopy air temperatures at night at Fraser) mean differences and RMS differences between needle-branch and air temperature-based exitances were double in the discontinuous Fraser stand compared to values at Marmot, with intermediate values at the uniform Fraser stand (Table II).

Substantial differences were found between trunk and air temperature-derived exitances with the largest differences of  $76\text{--}226 \text{ W m}^{-2}$  corresponding to periods of day time heating resulting from increased shortwave extinction. Decreased differences of  $20\text{--}30 \text{ W m}^{-2}$ , between exitances were observed on cold, clear nights due to trunks remaining warm throughout the night. As a result, mean differences in exitance between trunk and air temperature-derived values varied from 10 to  $24 \text{ W m}^{-2}$  over the range of conditions with RMS differences of  $15\text{--}50 \text{ W m}^{-2}$ . Tree trunks were not observed to remain cold during the day due to thermal lag, though this has been observed in dense northern boreal forests during melt (Sicart *et al.*, 2004) and might be expected in these sub-alpine forests in the low insolation, cold mid-winter period.

#### ESTIMATING SUB-CANOPY LONGWAVE IRRADIANCE

A re-analysis of data collected by Pomeroy and Dion (1996) at half-hourly intervals (562 measurements with regularly cleaned radiometers over and under a boreal pine stand near Waskesiu, Saskatchewan, Canada in winter 1993–1994) and inversion of Equation 7 with  $LAI' = 2.2$ , provides for a simple empirical relationship between extinction efficiency,  $Q_{\text{ext}}$ , and solar elevation angle above the horizon,  $\beta$ , that is more robust than the relationship developed from daily values as proposed by Pomeroy and Dion (1996),

$$Q_{\text{ext}} = 1.081\beta \cos(\beta), \quad r^2 = 0.85 \quad (8)$$

The observations and form of Equation 8 are shown in Figure 4.

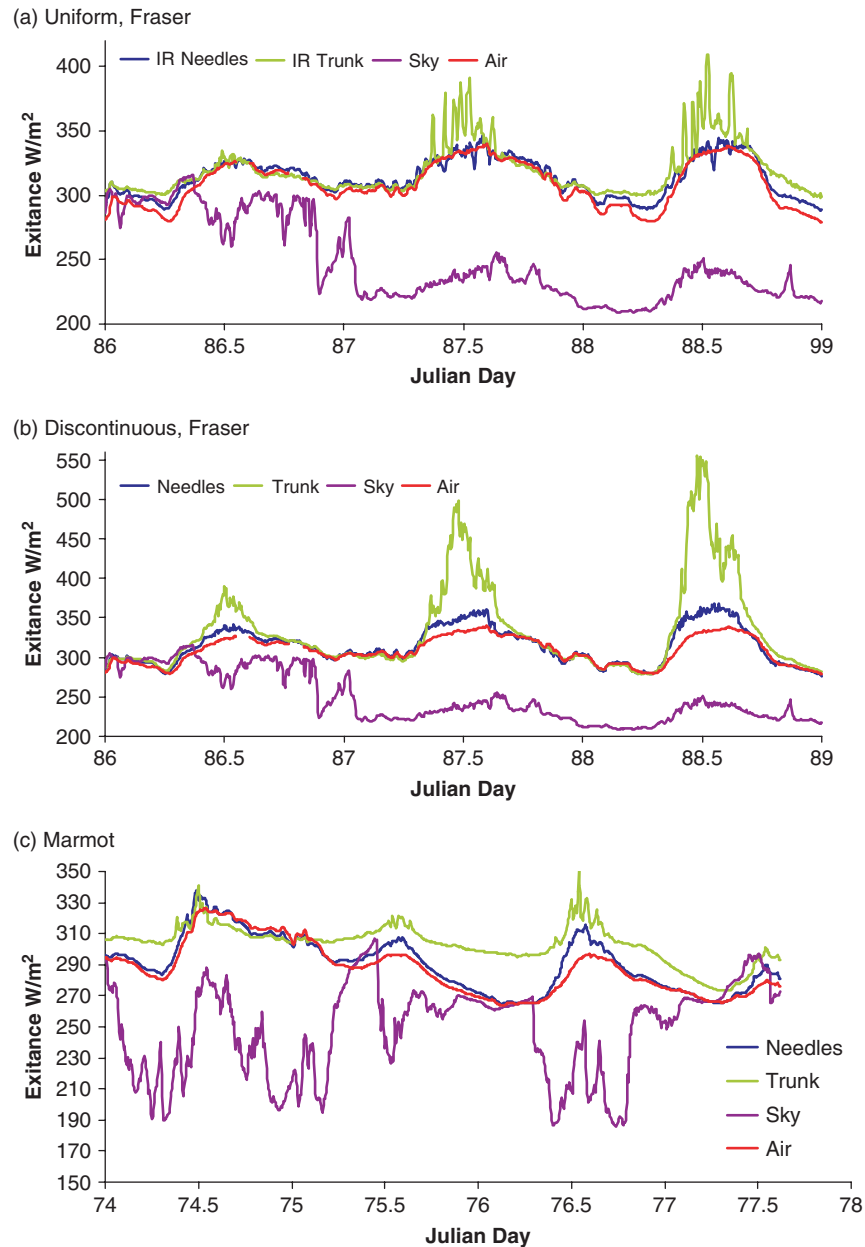


Figure 3. Longwave exitance from sky (measured) and estimated with emissivity of 0.98 from measured temperatures of needle-branches, trunk and sub-canopy air. (a) Fraser uniform canopy, (b) Fraser discontinuous canopy, (c) Marmot Creek

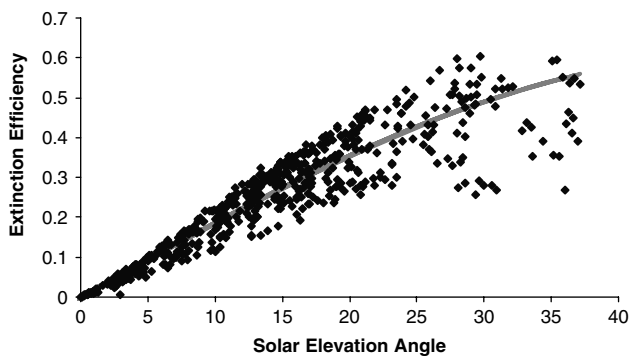


Figure 4. Winter 1993–1994 Waskesiu Pine Site. Modelled extinction efficiency from solar elevation angle (line) and that estimated from observations (points)

Pomeroy *et al.* (1997) collected radiation data using the same techniques as Pomeroy and Dion (1996) for several subsequent years at the same site. Using shortwave radiation observations and measured  $LAI'$ , Equations 5, 6, and 7 were used to estimate  $K^*_H$  for a 3-month winter period in 1995. The results suggest that the method is stable and sufficiently reliable to estimate canopy extinction of radiation (Figure 5). Unfortunately, reliable incoming longwave radiation and canopy temperatures were not available from this experiment, and so the direct influence of shortwave extinction on sub-canopy longwave irradiance could not be estimated at the time. This function was therefore tested at the Marmot and Fraser forests.

Irradiance to the snow surface was modelled in three manners, each having differing assumptions, data and parameter requirements.

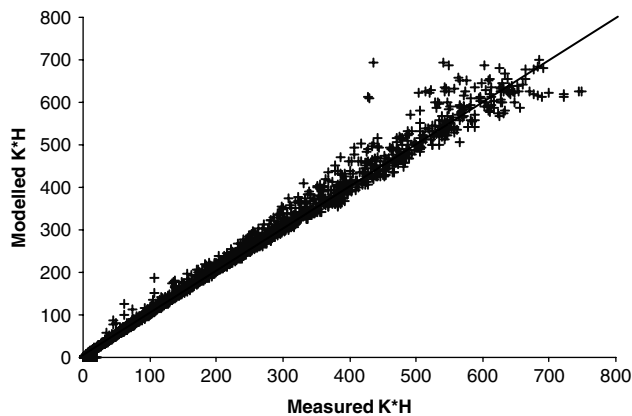


Figure 5. Modelled and measured  $K^*_H$ , calculated using a canopy albedo of 0.12 and snow albedo of 0.8 and LAI = 2.2. Based on 4260 half-hourly measurements of radiant flux above and below a pine canopy, Waskesiu, Saskatchewan, Canada 1995

1. Assuming that downwelling thermal radiation derives from only two sources, sky and canopy and that the sub-canopy air temperature can be taken as equal to the mean canopy temperature (Equation 3).
2. Assuming that downwelling thermal radiation derives from three distinctive thermal surfaces: sky, needle-branches and trunk. The observed spatial variability of canopy temperature shown in Figure 1 is assumed to be primarily captured by segregating the canopy into needles-branches and trunk elements, without further division into sunlit and shaded canopy portions. An equation describing this is:

$$L \downarrow = V_f \sigma \varepsilon_a T_a^4 + (1 - V_f) [(n_f \sigma \varepsilon_n T_n^4) + ((1 - n_f) \sigma \varepsilon_t T_t^4)]. \quad (9)$$

Where  $n_f$  is the needle-branch fraction of the canopy, i.e. the proportion of the canopy view that is needle-branches (from 0 to 1) and where the subscripts  $n$  and  $t$  denote the needle-branch and trunk components of the canopy. Note that if the air temperature is used in substitute for needle-branch temperature when  $n_f$  approaches 1.0, then Equation 9 approaches Equation 3 in its behaviour.

3. Assuming that downwelling thermal radiation derives from three energy sources, sky longwave irradiance, irradiance due to canopy elements at the air temperature, and irradiance due to canopy elements heated above the air temperature by extinction of shortwave radiation, where,

$$L \downarrow = \sigma T_a^4 (V_f \varepsilon_{\text{air}} + (1 - V_f) \varepsilon_{\text{can}}) + B K^*_H. \quad (10)$$

And  $\varepsilon_{\text{air}}$  represents the emissivity of the sky.

The three models were evaluated in the following manner. The sky view fraction and transmissivity were estimated using the diffuse shortwave transmissivity measured with arrays of Eppley shortwave radiometers (10–12 radiometers) at each site and a reference open sky site. However the needle-branch fraction of the canopy

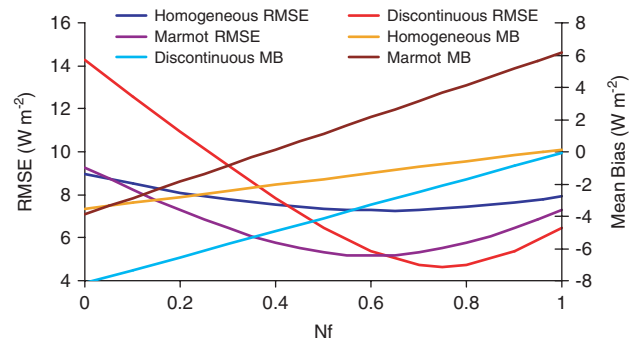


Figure 6. Root mean square error (RMSE) and mean bias (MB) of Equation 9 with varying needle-branch fraction of canopy for the three stands. Measured needle-branch and trunk temperatures were used along with measured sky exitance and sky view fraction

could not be measured directly. The parameter  $n_f$  was estimated by assuming that Equation 9 was correct and using measured needle-branch, trunk temperatures and sky longwave exitance and Equation 9 to estimate sub-canopy longwave irradiance. Figure 6 shows the RMS error and mean bias for Equation 9 using measured values and varying the needle-branch fraction of canopy. The minimum RMS error was found for needle-branch fractions between 0.6 and 0.75, however the smallest mean bias was found for needle-branch fractions of  $\sim 1$  (Fraser stands) and 0.3 (Marmot). Further modelling used minimized RMS error to select the needle-branch fraction, in an effort to most effectively simulate the effect of heating of the trunk and needle-branch canopy elements above air temperature.

The dimensionless shortwave to longwave transfer efficiency function,  $B$ , in Equation 4 is unknown and so was investigated at the sites by solving for  $B$  from measured  $K^*_H$  and measured components of Equation 10. The results are shown in Figure 7 and from the slope of the relationship between  $K^*_H$  and the difference between longwave irradiance predicted by Equation 3 (sky irradiance and air temperature based) and that measured, the best fit value of  $B$  for both Fraser sites was 0.023. The optimal value of  $B$  for each site differed only slightly from the overall best fit, being 0.020 ( $R^2 = 0.75$ ) for the uniform and 0.026 ( $R^2 = 0.71$ ) for the discontinuous stand. This difference may reflect greater transfer efficiency of absorbed shortwave energy to downward emissions of longwave in more sparse stands. However, given the scatter in the results the overall value of 0.023 was used in subsequent modelling. For Marmot, the best fit value was 0.023 ( $R^2 = 0.59$ ), in correspondence with the Fraser sites, however an offset occurred in Marmot of  $5 \text{ W m}^{-2}$  due to trees remaining warm relative to the air at night such that  $B$  did not approach zero when solar irradiance did. Forcing  $B$  through zero resulted in a value of 0.038 and preserved model simplicity but with a much lower  $R^2$  of 0.25. Of interest is the wide scatter in the ratio  $B$  (slope in Figure 7) for high values of solar extinction at Fraser. Given the time of year (end of March) and low latitude ( $39^\circ \text{N}$ ) compared to Marmot (mid March,  $51^\circ \text{N}$ ) the solar elevation angle above the horizon would

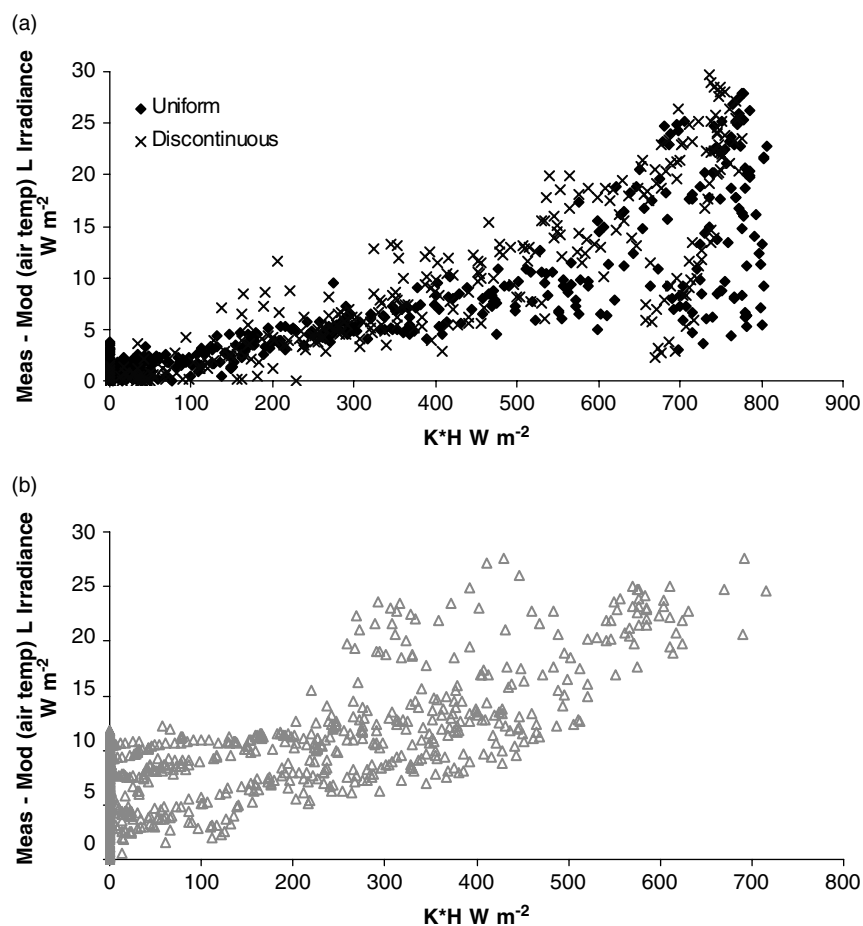


Figure 7. The net extinction of shortwave radiation in pine canopy and the difference between longwave irradiance predicted by Equation 3 (sky irradiance and air temperature based) and that measured for (a) Fraser uniform (point) and discontinuous ( $\times$ ) stands and (b) the Marmot stand

be much higher at Fraser than at Marmot. At the highest irradiances the extinction of beam radiation by trunks might have been relatively smaller for the high elevation angles that are been associated with the highest irradiance values.

Using measured sky irradiance and models (i) air temperature = canopy temperature (Equation 3), (ii) measured needle-branch and trunk temperatures (Equation 9) with the 'best fit' values of needle-branch fraction with respect to RMS error (0.65, 0.75, 0.60, respectively, for the uniform and discontinuous Fraser stands, and the Marmot stand), and (iii) air temperature and estimated shortwave extinction in the canopy with  $B = 0.023$  for Fraser and  $B = 0.038$  for Marmot (Equation 10), the longwave irradiance was calculated for the three field sites (Figure 8). The highest RMS errors and mean bias were from the air temperature model (Equation 3); it should be noted that most of the errors accumulated during periods of strong insolation. Better performances were from either the needle-branch and trunk temperature model (Equation 8) or the air temperature and shortwave extinction model (Equation 10). RMS errors were not notably reduced from the air temperature model by using trunk and needle-branch temperatures at the Fraser uniform site but they were reduced in half by adding this component in the discontinuous stand at

Fraser and at the Marmot stand (Table III). Incorporating trunk and needle-branch temperatures or shortwave extinction at all sites reduced mean bias by up to four-fold compared to the air temperature based model.

#### SENSITIVITY OF LONGWAVE IRRADIANCE TO SOLAR HEATING OF CANOPY

In order to better describe how the enhancement of longwave radiation to snow from solar heating varies with forest density, solar elevation angle and air temperature conditions, a model, based on the shortwave extinction enhancement of longwave model (iii), was constructed for the purposes of sensitivity analysis. The model assumes clear sky conditions with an atmospheric emissivity of 0.6 and vegetation emissivity of 0.98. The variables driving the model are solar elevation angle, air temperature, and effective leaf area index, whilst the parameters are emissivity, albedos of forest and snow and  $B$ . To estimate the shortwave irradiance to a flat surface the model uses a linear approximation of the relationship between solar elevation angle and shortwave irradiance in mid-March as calculated using physically based algorithms in the Cold Regions Hydrological Model (Pomeroy *et al.*, 2007). The approximation is valid

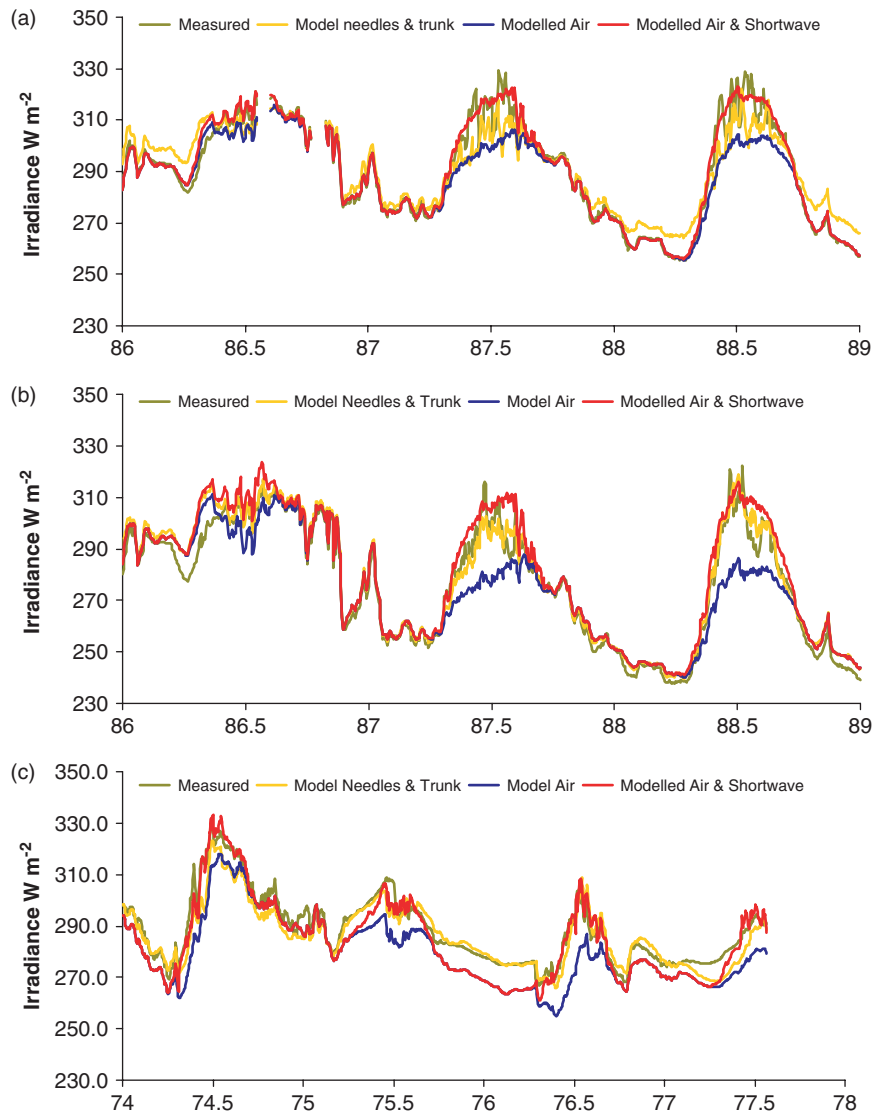


Figure 8. Modelled and measured irradiance at the uniform Fraser stand (a), discontinuous Fraser stand (b) and Marmot stand (c), using above canopy irradiance and model (i) air temperature only (Equation 3), (ii) needle-branch and trunk temperatures with optimized needle-branch fraction (Equation 9), and (iii) air temperature and shortwave extinction with optimized efficiency function (Equation 10)

Table III. Errors in estimation of longwave irradiance to snow for three sites

	Air temperature		Needle-branch-trunk		Air and shortwave extinction	
	RMS error	Mean bias	RMS error	Mean bias	RMS error	Mean bias
Fraser uniform	7.03	5.49	7.28	-1.13	3.26	-0.80
Fraser discontinuous	9.24	3.58	4.66	-2.09	4.91	-1.61
Marmot Creek	10.13	8.70	5.17	2.16	5.84	4.04

Model (i) (air temperature) uses Equation 3, Models (ii) and (iii) use Equation 4 with (ii) measured needle-branch and trunk temperatures and (iii) air temperature as an estimate of needle-branch temperature and measured trunk temperatures.

from at least 30° to 55°N ( $r^2 = 0.99$ ) and is,

$$K \downarrow = 1040 \beta \tag{11}$$

where  $\beta$  is given in radians and the coefficient 1040 has units of  $W m^{-2}$ . The model also uses the empirical relationship between  $LAI'$  and the sky view factor,  $V_f$ ,

for conifer canopies given by Pomeroy *et al.* (2002);

$$V_f = 0.45 - 0.29 \ln(LAI') \tag{12}$$

The model then uses Equations 6–8, and 10–12 to estimate the longwave irradiance to snow.

Results of the model assuming the albedo of forest is 0.12, the albedo of snow under the forest is 0.8 and  $B$  is 0.023 are shown in Figure 9 for the range

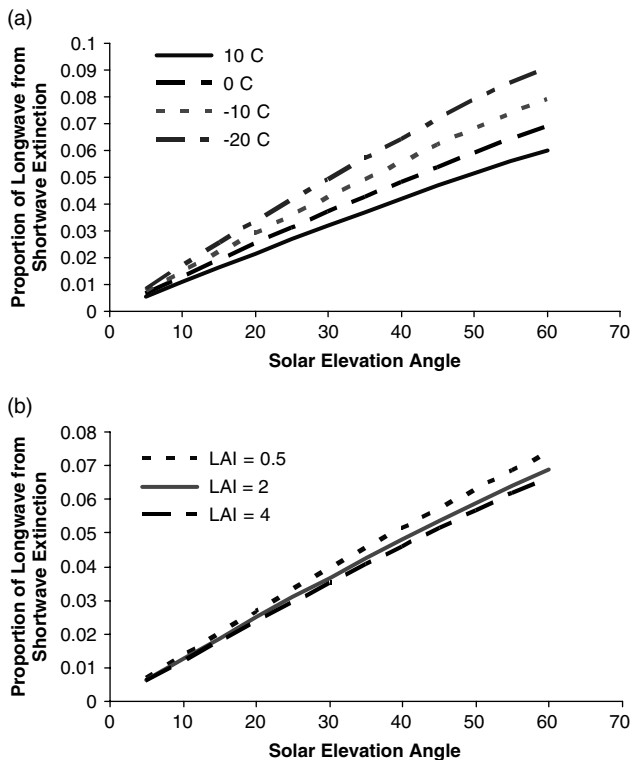


Figure 9. Ratio of modelled enhanced downwelling longwave due to shortwave extinction in the canopy to total longwave irradiance to snow. (a) as a function of air temperature and solar elevation angle for  $LAI' = 2$ . (b) as a function of effective winter leaf area index and solar elevation angle for an air temperature of  $0^{\circ}\text{C}$

of solar elevation angles that are found during premelt and melt periods in the Rocky Mountains. Note that the contribution of enhanced longwave from solar extinction ( $B K^*_{\text{H}}$ ) approximately doubles if the value of  $B$  from Marmot Creek is chosen instead of the more conservative value from Fraser. Figure 9a shows the ratio of longwave due to shortwave extinction to total longwave irradiance to snow as a function of solar elevation angle and air temperature for a fixed  $LAI' = 2$ . It is apparent that the enhancement of longwave due to shortwave extinction in the canopy is significant at higher solar elevation angles; this enhancement amounts up to about 9%, or about  $20 \text{ W m}^{-2}$  on average, of longwave irradiance to snow under cold conditions. Note that using the Marmot value of  $B$  (0.038) results in a maximum longwave enhancement of  $30 \text{ W m}^{-2}$  or about 15% of longwave irradiance to snow at  $-20^{\circ}\text{C}$  air temperature and an elevation angle of  $60^{\circ}$ . As air temperature increases, the magnitude of this contribution does not drop, but its importance does such that it is only 6% of longwave irradiance to snow at  $+10^{\circ}\text{C}$  and high solar elevation angles ( $60^{\circ}$ ). Figure 9b shows the effect of varying effective leaf area index on the ratio of longwave due to shortwave extinction to total longwave irradiance for a fixed air temperature of  $0^{\circ}\text{C}$ . There is relatively little sensitivity to  $LAI'$  because greater  $LAI'$  results in both greater extinction of shortwave, which is partially converted to downwelling longwave and a smaller sky view factor which results in greater canopy contribution to downwelling longwave. The two

increases in longwave irradiance are largely matched though there is slightly greater relative contribution from shortwave extinction at lower canopy densities.

These model results help explain why Sicart *et al.* (2004) did not observe enhancement of longwave due to shortwave extinction in the Yukon sub-arctic where low solar elevation angles during melt would have limited the magnitude of  $B K^*_{\text{H}}$ . Similarly, the effect is expected to be small during mid-winter at higher latitudes of Canada when solar elevation angles are always quite low. However it can be important over much of the winter for the southern Rocky Mountains in the United States. The insensitivity of this longwave enhancement due to shortwave extinction effect to forest density suggests that it is equally important in a wide range of coniferous forest densities and that forest management cannot be used to accelerate snowmelt by this effect (though, in general, forest density has a strong effect on longwave irradiance under clear skies). The model does not account for effects such as percentage of dead trees, which may have an important effect on the value of  $B$ . This factor urgently needs further research as the pine forests of the Rocky Mountains are currently being subjected to mountain pine beetle infestations and fire-induced mortality, such that the effect of standing dead timber on longwave radiation is of immense practical importance for calculating the change in snowmelt rate and timing with forest cover change.

## CONCLUSIONS

This study has shown that the assumption of equality between air temperature and canopy temperatures is not always met, and that above canopy and especially sub-canopy temperatures are often colder than canopy temperatures under strong insolation. There is a substantial variability to canopy surface temperatures and enhancement of these surface temperatures above the air temperature due to extinction of solar radiation. The failure of the assumption of canopy and air temperature equality can lead to substantial differences between estimates and measurements of sub-canopy longwave irradiance to snow during sunlit periods, if sub-canopy irradiance is estimated using only air temperature, sky view factor and above canopy longwave irradiance. Sunlit tree trunks were substantially warmer than air temperature and sunlit needle-branches, which were sometimes warmer than air temperature. The largest differences occurred for situations with strong insolation to discontinuous canopies where small gaps permitted shortwave radiation to be extinguished well down within the canopy. Smaller differences between estimates and measurements occurred for all canopies at night and during cloudy periods, and for uniform canopies in general.

The extinction of shortwave radiation led directly to canopy warming and hence to persistent differences in the canopy longwave exitance calculated using only air temperature from those measured. It is therefore suggested that estimates of sub-canopy longwave irradiance

use two-component approaches to evaluate the contribution of canopy longwave exitance. The two-energy component approach uses a combination of air temperature and shortwave extinction by canopy to estimate the canopy longwave exitance. The two-thermal regime approach partitions the canopy between needle-branch exitance and trunk exitance with explicit observations or calculations of trunk and needle-branch temperature to drive the exitance calculations. For situations where the canopy temperature is not directly measured or correctly modelled then the two-energy component approach provides a relatively simple method to estimate the enhanced canopy longwave exitance using only canopy characteristics, air temperature and shortwave extinction. During conditions that are common during snowmelt at high and low latitude sites in the Rocky Mountains of the US and Canada there was little evidence that such corrections are necessary under cloudy periods. However, when direct sunlight was extinguished by the canopy, the effect was very important to the magnitude of longwave irradiance to snow with longwave. Enhance of longwave irradiance to snow ranged up to  $30 \text{ W m}^{-2}$ . The relative importance of this longwave enhancement effect was greatest at high solar elevation angles and cold air temperatures. There was little influence of forest density on the relative importance of longwave enhancement from shortwave extinction because both shortwave extinction and canopy contribution to downwelling longwave increased with leaf area index. The presence of dead trees may have increased the magnitude of the longwave enhancement effect but requires further research. Because of the persistence of longwave enhancement from shortwave extinction over long periods, it is expected that inclusion of this enhancement in energy balance models of snowmelt will improve their performance in forested environments.

#### ACKNOWLEDGEMENTS

The authors would like to acknowledge the assistance of Mike Solohub (University of Saskatchewan), Kelly Elder and Manuel Martinez (USDA Forest Service) with research site operations, field observations and instrument deployment. The assistance of Richard Essery of Edinburgh University to all aspects of this project is gratefully acknowledged. The financial support of NOAA, NERC, NSERC, CFCAS (IP3), US Army Corps of Engineers, the Canada Research Chair Programme, and the home institutions of the authors is gratefully appreciated. Logistical support of the Nakiska Ski Area and Biogeoscience Institute (University of Calgary) for Marmot Creek research and USDA Forest Service for Fraser Experimental Forest research is appreciated.

#### REFERENCES

- Betts AK, Ball JH. 1997. Albedo over the boreal forest. *Journal of Geophysical Research* **102**: 28901–28909.  
 Davis RE, Hardy JP, Ni W, Woodcock C, McKenzie CJ, Jordan R, Li X. 1997. Variation of snow cover ablation in the boreal forest: a sensitivity

- study on the effects of a conifer canopy. *Journal of Geophysical Research* **102**(D24): 29389–29395.  
 Ellis CR, Pomeroy JW. 2007. Estimating sub-canopy shortwave irradiance to melting snow on forested slopes. *Hydrological Processes* **21**: 2581–2593.  
 Faria DA, Pomeroy JW, Essery RLH. 2000. Effect of covariance between ablation and snow water equivalent on depletion of snow-covered area in a forest. *Hydrological Processes* **14**: 2683–2695.  
 Gryning S-E, Batchvarova E, de Bruin HAR. 2001. Energy balance of a sparse coniferous high-latitude forest under winter conditions. *Boundary Layer Meteorology* **99**: 465–488.  
 Harding RJ, Pomeroy JW. 1996. The energy balance of the winter boreal landscape. *Journal of Climate* **9**: 2778–2787.  
 Hardy JP, Davis RE, Jordan R, Li X, Woodcock C, Ni W, McKenzie JC. 1997. Snow ablation modelling at the stand scale in a boreal jack pine forest. *Journal of Geophysical Research* **102**(N24): 29397–29406.  
 Hardy JP, Melloh RA, Koenig G, Marks D, Winstral A, Pomeroy JW, Link T. 2004. Solar radiation transmission through conifer canopies. *Agricultural and Forest Meteorology* **126**: 257–270.  
 Hardy JP, Davis RE, Koh Y, Cline D, Elder K, Armstrong R, Marshall H-P, Painter T, Castres G, DeRoo R, Sarabandi K, Graf T, Koike T, McDonald K. 2008. NASA Cold Land Processes Experiment (CLPX 2002–2003): Local Scale Observation Site (LSOS). *Journal of Hydrometeorology* **9**(6): 1434–1442.  
 Link TE, Marks D. 1999. Point simulation of seasonal snow cover dynamics beneath boreal forest canopies. *J. Geophys. Res.* **104**: 27841–27857.  
 Link TE, Marks D, Hardy J. 2004. A deterministic method to characterize canopy radiative transfer properties. *Hydrol. Process* **18**: 3583–3594.  
 Marks D, Domingo J, Susong D, Link T, Garen D. 1999. A spatially distributed energy balance snowmelt model for application in mountain basins. *Hydrological Processes* **13**(13–14): 1935–1959.  
 Marks D, Reba M, Pomeroy J, Link T, Winstral A, Flerchinger G, Elder K. 2008. Comparing simulated and measured sensible and latent heat fluxes over snow under a pine canopy. *Journal of Hydrometeorology* **9**(6): 1506–1522.  
 Melloh RA, Hardy JP, Bailey RN, Hall TJ. 2002. An efficient snow albedo model for the open and sub-canopy. *Hydrol. Process.* **16**: 3571–3584.  
 Ni W, Li X, Woodcock C, Roujean J-L, Davis RE. 1997. Transmission of solar radiation in boreal conifer forests: Measurements and models. *Journal of Geophysical Research* **102**(D24): 29555–29566.  
 Nijssen B, Lettenmaier DP. 1999. A simplified approach for predicting shortwave radiation transfer through boreal forest canopies. *Journal of Geophysical Research* **104**: 27859–27868.  
 Oke TR. 1987. *Boundary Layer Climates*. Routledge: New York; 435 pp.  
 Parviainen J, Pomeroy JW. 2000. Multiple-scale modelling of forest snow sublimation: initial findings. *Hydrological Processes* **14**: 2669–2681.  
 Pomeroy JW, Dion K. 1996. Winter irradiance extinction and reflection in a boreal pine canopy: measurements and modelling. *Hydrological Processes* **10**: 1591–1608.  
 Pomeroy JW, Granger RJ. 1997. Sustainability of the western Canadian boreal forest under changing hydrological conditions—I- snow accumulation and ablation. In *Sustainability of Water Resources under Increasing Uncertainty*, D. Rosjberg, N. Boutayeb, A. Gustard, Z. Kundzewicz and P Rasmussen (eds). IAHS Publ No. 240. IAHS Press: Wallingford, UK; 237–242.  
 Pomeroy JW, Granger RJ, Pietroniro A, Elliott JE, Toth B, Hedstrom N. 1997. Hydrological Pathways in the Prince Albert Model Forest: Final Report. NHRI Contribution Series No. CS-97007. 153 p. plus append. Available at <http://mfliq.sasktelwebhosting.com/pubs/PAMF3400.pdf>.  
 Pomeroy JW, Gray DM, Hedstrom NR, Janowicz JR. 2002. Prediction of seasonal snow accumulation in cold climate forests. *Hydrological Processes* **16**: 3543–3558.  
 Pomeroy JW, Bewley DS, Essery RLH, Hedstrom NR, Link T, Granger RJ, Sicart JE, Ellis CR, Janowicz JR. 2006. Shrub tundra snowmelt. *Hydrological Processes* **20**: 923–941.  
 Pomeroy JW, Gray DM, Brown T, Hedstrom NH, Quinton WL, Granger RJ, Carey SK. 2007. The cold regions hydrological model: a platform for basing process representation and model structure on physical evidence. *Hydrological Processes* **21**: 2650–2667.  
 Pomeroy JW, Rowlands A, Hardy J, Link T, Marks D, Essery R, Sicart J-E, Ellis C. 2008. Spatial variability of shortwave irradiance for snowmelt in forests. *Journal of Hydrometeorology* **9**(6): 1482–1490.  
 Price AG, Petzold DE. 1984. Surface emissivities in a boreal forest during snowmelt. *Arctic Alpine Res.* **16**: 45–51.  
 Rowlands A, Pomeroy J, Hardy J, Marks D, Elder K, Melloh R. 2002. Small-scale spatial variability of radiant energy for snowmelt in a

- mid-latitude sub-alpine forest. Proceedings from the 59th *Eastern Snow Conference*. pp 109–117.
- Sicart J-E, Pomeroy JW, Essery RLH, Hardy J, Link T, Marks D. 2004. A sensitivity study of daytime net radiation during snowmelt to forest canopy and atmospheric conditions. *Journal of Hydrometeorology* **5**: 774–784.
- Sicart J-E, Pomeroy JW, Essery RLH, Bewley D. 2006. Incoming longwave radiation to melting snow: observations, sensitivity and estimation in northern environments. *Hydrological Processes* **20**: 3697–3708.
- Taylor CM, Harding RJ, Pielke RA, Pomeroy JW, Vidale PL, Walko RL. 1998. Snow breezes in the boreal forest. *Journal of Geophysical Research* **D18**(103): 23,087–23,103.
- van de Hulst. 1980. *Multiple Light Scattering*. Academic Press: New York; 739 pp.
- Verseghy D, McFarlane N, Lazare M. 1993. CLASS—A Canadian land surface scheme for GCM's, II. Vegetation model and coupled runs. *International Journal of Climatology* **13**(44): 347–370.
- Wilson RG, Petzold DE. 1973. A solar radiation model for sub-arctic woodlands. *J. Appl. Meteorol.* **12**: 1259–1266.
- Woo M, Giebrecht MA. 2000. Simulation of snowmelt in a subarctic spruce woodland: 1. Tree model. *Water Resources Research* **36**(8): 2275–2285.